Surface viscosity of liquid interfaces from Green–Kubo relations

Pál Jedlovszky 💿 ; Marcello Sega 🗷 💿



J. Chem. Phys. 160, 201101 (2024) https://doi.org/10.1063/5.0206954





Articles You May Be Interested In

Surface viscosity in simple liquids

J. Chem. Phys. (March 2023)

Time reversal symmetry breaking and odd viscosity in active fluids: Green-Kubo and NEMD results

J. Chem. Phys. (May 2020)

Non-local viscosity from the Green-Kubo formula

J. Chem. Phys. (May 2020)

Surface viscosity of liquid interfaces from Green-Kubo relations

Cite as: J. Chem. Phys. 160, 201101 (2024); doi: 10.1063/5.0206954

Submitted: 5 March 2024 • Accepted: 30 April 2024 •

Published Online: 22 May 2024









Pál Jedlovszky¹ D and Marcello Sega^{2,a)}



AFFILIATIONS

- Department of Chemistry, Eszterházy Károly Catholic University, Leányka Utca 12, H-3300 Eger, Hungary
- ² Department of Chemical Engineering, University College London, WC1E 7JE London, United Kingdom
- a) Author to whom correspondence should be addressed: m.sega@ucl.ac.uk

ABSTRACT

The precise determination of surface transport coefficients at liquid interfaces is critical to an array of processes, ranging from atmospheric chemistry to catalysis. Building on our prior results that highlighted the emergence of a greatly reduced surface viscosity in simple liquids via the dispersion relation of surface excitations [Malgaretti et al., J. Chem. Phys. 158, 114705 (2023)], this work introduces a different approach to directly measure surface viscosity. We use modified Green-Kubo relations suitable for inhomogeneous systems to accurately quantify viscosity contributions from fluid slabs of variable thickness through extensive molecular dynamics simulations. This approach distinguishes the viscosity effects of the surface layer vs the bulk, offering an independent measure of surface viscosity and providing a more detailed understanding of interfacial dynamics and its transport coefficients.

© 2024 Author(s). All article content, except where otherwise noted, is licensed under a Creative Commons Attribution (CC BY) license (https://creativecommons.org/licenses/by/4.0/). https://doi.org/10.1063/5.0206954

Chemical reactions that take place at liquid interfaces exhibit distinct kinetics and thermodynamics compared to those occurring in the bulk.¹⁻⁵ Understanding the behavior of these reactions is crucial for environmental,6 industrial,7 and biological processes, 8,9 yet it remains a challenge due to their complexity, including the determination of transport properties in the interfacial

Historical insights into surface viscosity can be traced back to the foundational contributions of Marangoni and Boussinesq, highlighting its significance in fluid dynamics at interfaces. 10-Traditionally, research into surface viscosity has focused on complex rheological systems, underlining its role in key phenomena, such as liquid film formation,13 droplet dynamics,14 and in general systems whose properties are dominated by the adsorption of surfactants.¹⁵ Interest in the surface viscosity of Newtonian fluids, notably water, re-emerged in the 1980s through experimental studies, 16 which later faced a re-evaluation, 17 partly due to methodological constraints that limited observations to micrometer-scale interfacial areas, thus missing the molecular-scale effects. The recent advances in computational methods and molecular dynamics simulations have revitalized this area of study, revealing the increased

mobility of molecules at the surface of simple liquids¹⁸ and suggesting a unique surface viscosity distinct from that in the bulk phase.¹⁹ This shift emphasizes the need for direct measurement methods that accurately reflect the complex behavior of surface viscosity and its impact at the molecular level.^{20,2}

In our previous work, we collected evidence of a surprisingly low surface viscosity in liquid argon by analyzing the dispersion law of surface modes using the linearized solution of the continuum hydrodynamic equations in the presence of an interface. The surface viscosity measured this way appears to be largely confined to the first molecular layer, with a bulk-like behavior, including propagation of sound waves already emerging in the second molecular layer. The mismatch between the molecular scale at which the surface viscosity appears and the macroscopic continuum modeling used to interpret the measured dispersion laws could be rightfully considered a limitation. For this reason, we decided to attack the problem using a different approach based on the fully microscopic Green-Kubo relations, modified to account for inhomogeneous systems. Here, we conduct an in-depth analysis of viscosity contributions within fluid layers of differing thicknesses through extensive molecular dynamics simulations. This method allows separating surface and bulk fluid shear viscosity, providing an independent measure of the surface viscosity.

Green-Kubo relations²² are routinely used to extract transport coefficients by exploiting equilibrium fluctuations, including shear viscosity. In bulk systems, the shear viscosity can be computed via the integral of the autocorrelation function of off-diagonal pressure tensor elements, although other non-equilibrium approaches might be more efficient.²³ For inhomogeneous systems, the simple Green-Kubo formula would not suffice, and in principle, the non-locality of the associated response function should be considered,²⁴ although the required amount of sampling in an inhomogeneous setting would be prohibitive. Since far from the critical point, the liquid phase presents a rather sharp transition to the vapor, with inhomogeneity confined to, at most, the first three molecular layers close to the surface,25 we use the following approximation, valid for single-component fluids, in which we replace the volumes appearing in the definition of the pressure tensor elements and in the Green-Kubo formulas by the equivalent volume $V = N/\rho$ occupied by N molecules. Here, ρ is the density far from the interface in a system in slab configuration with a large number of particles, where finite size effects are supposed to be negligible. This way, the pressure tensor reads $\mathbf{p} = 2N(\mathbf{T})$ $-\Xi$)/ ρ , where $\mathbf{T} = \sum_{i} m_{i} \mathbf{v}_{i} \otimes \mathbf{v}_{i}/2$ is the kinetic energy tensor and $\Xi = \sum_i \mathbf{F}_i \otimes \mathbf{r}_i / 2$ is the virial tensor for particles with position \mathbf{r}_i and velocity \mathbf{v}_i subject to a force \mathbf{F}_i . Similarly, the Green-Kubo relation for the (average) viscosity of an inhomogeneous system can be written as

$$\eta = \lim_{t \to \infty} (N/\rho) \int_0^{t_f} \langle p_{xy}(0) p_{xy}(t) \rangle dt, \tag{1}$$

where, once more, the definition of the pressure tensor is the one described above, which uses the effective volume of the liquid phase. Here, we assume that the liquid–vapor interfacial system is in a slab configuration with its normal directed along z. In this case, the momentum can freely diffuse, under periodic boundary conditions, along the x and y directions, which are those appearing in the formula for η .

The key approximation that we use to extract the surface viscosity is to consider a two-layer model, where the fluid slab of thickness h is regarded as the stacking of two interfacial regions of thickness h_s and viscosity η_s and one region of thickness $h - 2h_s$ and viscosity η_0 . The total viscosity of a slab system can then be approximated as the average of η_0 and η_s , weighted by the respective volumes,

$$\eta(h) = [\eta_0(h - 2h_s) + \eta_s 2h_s]/h,$$
(2)

very much in the spirit of the approach that Lyman and coworkers used for lipid membranes. 9,26 The difference in this case is that there is only one component and two phases, and one needs to use the Green–Kubo relation adapted for inhomogeneous systems, as described before. The main idea is to simulate liquid–vapor equilibrium systems of varying thickness and extract the surface viscosity η_s from a best-fit procedure. Given the number of particles N in the system, we can use the corresponding effective thickness, $h=N/(A\rho)$, where A is the simulation box cross-sectional area.

We performed a series of molecular dynamics simulations of liquid argon, using the Lennard-Jones interaction potential $U(r) = 4\epsilon \left[(\sigma/r)^{12} - (\sigma/r)^6 \right]$ with $\epsilon = 0.99641$ kJ/mol and

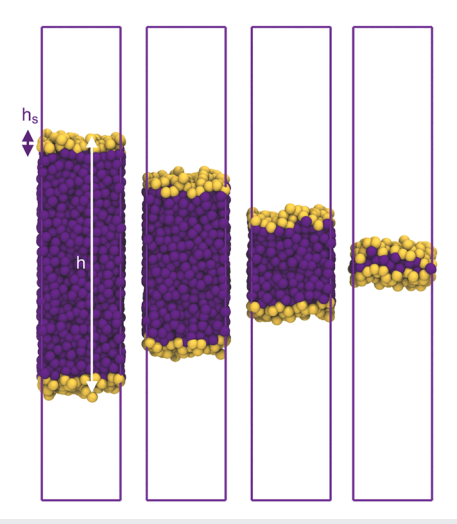


FIG. 1. Simulation snapshots of the argon system, with surface layer atoms highlighted in yellow. From left to right, the largest system with N=3000, two intermediate ones (N=2119 and 1207), and the smallest stable 2d-spanning system, with N=400 atoms. The simulation box is also represented with a thin frame.

 $\sigma = 0.340\,98$ nm at the temperature of 90 K using the GRO-MACS²⁷ simulation package, version 2023.0, integrating the equations of motion with a time step of 1 fs in the canonical ensemble (Nosè-Hoover thermostat^{28,29} with a time constant of 2 ps), taking into account the long-range interaction effects^{30,31} with the smooth particle mesh Ewald method³² (using a real-space cutoff of 1.3 nm, a Fourier spacing of 0.15 nm, and a relative contribution of the realspace part of the potential at cutoff of 0.001). We simulated systems with the number of argon atoms N ranging from 400 to 3000 in a rectangular box with edges 3.6014, 3.6014, and 21.6 nm, in slab configuration with normal along the z direction. Figure 1 shows some equilibrated configurations. We integrated the equations of motion for at least 50 ns for each system, dumping to disk the values of the pressure tensor elements every 1 fs and the configurations every 10 ps. We computed the autocorrelation functions using a fast Fourier transform approach, exploiting the complete information encoded in the dumped data.

Figure 2 shows the measured viscosity as a function of the effective slab thickness h. The viscosity was obtained by averaging the value of the integral, Eq. (1), over 1000 points in the range t_f from 4 to 5 ps, where it has reached a clear plateau of the running Green–Kubo integral $\eta(t_f)$ for all systems, as shown in Fig. 3. The length of the simulations (at least 50 ns) and the frequency of dumping the pressure tensor components (1 fs) were key to reach the high accuracy shown in Figs. 2 and 3.

Simulations with an effective thickness h < 1.2 nm were too small in size to stably span the simulation box in two directions, collapsing into cylindrical droplets, spherical droplets, or transitioning completely to the gas phase. At larger values of h, the measured viscosity shows a clear increasing trend that reaches an asymptotic value for large values of the effective thickness.

By recasting the viscosity expression in the form $h\eta(h) = \eta_0 h - 2\Delta \eta h_s$, with $\Delta \eta = \eta_0 - \eta_s$, it becomes clear that there is no chance

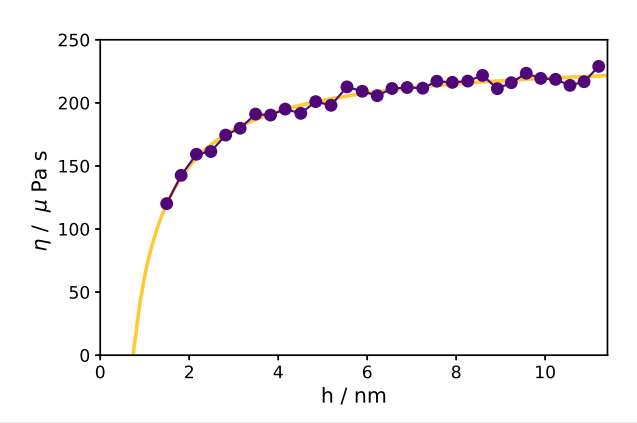


FIG. 2. Thickness-dependent viscosity $\eta(h)$ (circles) measured for systems with particle numbers ranging from 400 to 3000, as a function of the effective thickness $h = N/(A\rho)$. The continuous line is the best fit for the two-layer model, Eq. (2).

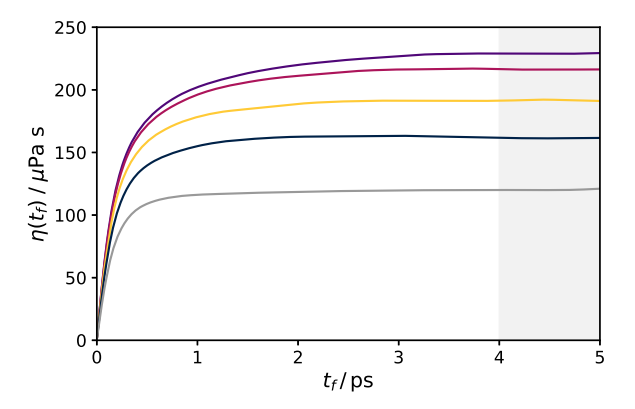


FIG. 3. Running Green–Kubo integral $\eta(t_f)$ from Eq. (1), for the same selected set of thicknesses shown in Fig. 1 (from the top to the bottom, N = 3000, 2119, 1207, and 400, respectively). The shaded area represents the region over which the integral is averaged to obtain the reported estimates.

to independently determine the two parameters η_s and h_s from a fit, as any combination that gives the same product will yield the same best fit. Luckily, we can obtain an estimate of the equivalent thickness of the surface layer h_s by using the surface molecule identification algorithm GITIM,³³ as implemented in the Pytim software package, 34 to count how many molecules N_s belong to each of the surface layers. We can then estimate the equivalent height from the bulk density and the simulation box cross-sectional area A as h_s = $N_s/(A\rho)$. The first step to obtaining N_s involves identifying the liquid phase as the largest cluster of atoms (two particles are considered to be in the same cluster if their distance is less than 0.45 nm). Then, we applied the GITIM algorithm, which, in a nutshell, computes the Delaunay triangulation of the atomic positions to determine all interstitial spaces between atoms and tags as surface ones, the atoms at the vertices of triangles that can host a probe sphere with radius r_p , also taking the atomic excluded volumes into account. To choose the probe radius $r_p = 0.195$ nm, we followed the prescription described in Ref. 35.

This calculation yields a mean number of surface layer atoms on each side of the slab equal to $N_s=114\pm1$, corresponding to an effective thickness of the interfacial layer $h_s=0.43$ nm. The value of h_s is larger than $\sigma=0.340\,98$ as it characterizes an interfacial layer that is corrugated at a scale below that of capillary waves, 35 but is still comparable to the molecular size. Keeping this parameter fixed, we could proceed with the best fit of the two-layer model, providing, as the main result of this work, the estimate of the viscosity and surface viscosity $\eta_0=237\pm2$ and $\eta_s=32\pm6\,\mu\text{Pa}$ s, respectively.

Interestingly, the smallest system that can stably span the xy cross section of the simulation box is composed, as shown in Fig. 1, of three layers only, namely, two surface layers and an inner layer. What is quite impressive, in our opinion, is that the best fit describes very well the behavior of the $\eta(h)$ curve up to the smallest stable system, showing that the two-layer model can capture the phenomenology of the surface viscosity down to systems consisting of a single molecular layer surrounded by two surface ones.

The resulting fit parameter η_0 is the extrapolation to an infinitely thick slab of fluid and agrees with the value of 240 μPa s provided by the model viscosity of argon that matches the experimental data within 2%.³⁶ The calculation of the surface viscosity considerably improves our previous estimate obtained using the surface modes dispersion relations, 19 which was roughly a factor 8 – 16 times smaller than the shear viscosity of the bulk fluid, corresponding in this case to the range $\eta_s = 15 - 30 \mu Pa$ s. In our previous work, it was not possible to provide a quantitative estimate of the uncertainty, and the range we provided was based on a qualitative assessment, while with the present approach, we can provide a quantitative prediction. The surface viscosity η_s is still several (6-9)times smaller than the shear viscosity of the bulk fluid, providing an independent confirmation of a greatly reduced surface viscosity. It is worth mentioning that the estimate of η_s depends on h_s , and any change in the thickness of the surface layer would reflect on the value of the surface viscosity. However, a reasonable $\pm 10\%$ change in h_s yields surface viscosity estimates in the range 11–50 μ Pa s, still confirming a markedly reduced surface transport coefficient.

In conclusion, this work introduces a novel approach for directly measuring surface viscosity, leveraging modified Green–Kubo relations within the framework of inhomogeneous systems. Using extensive molecular dynamics simulations, we have demonstrated the existence of a greatly reduced surface viscosity in liquid argon, which is a general model for simple liquids. This study opens several avenues for further research, particularly in exploring the surface viscosity of different fluids and their impact on various physical and chemical processes. The methodology can be applied as-is to other neat liquids of practical importance, such as water, taking care of calculating the pressure contribution on a molecular rather than on an atomic basis, potentially leading to a broader understanding of surface phenomena and interfacial dynamics. The application of this method to other liquids is already underway.

P.J. acknowledges financial support from the Hungarian NKFIH Foundation under Project No. 134596.

AUTHOR DECLARATIONS

Conflict of Interest

The authors have no conflicts to disclose.

Author Contributions

Pál Jedlovszky: Conceptualization (supporting); Methodology (supporting); Writing – original draft (supporting); **Marcello Sega**: Conceptualization (lead); Methodology (lead); Writing – original draft (lead).

DATA AVAILABILITY

The data that support the findings of this study are available from the corresponding author upon reasonable request.

REFERENCES

- ¹ A. Chanda and V. V. Fokin, Chem. Rev. **109**, 725 (2009).
- ²P. Jungwirth and D. J. Tobias, Chem. Rev. **106**, 1259 (2006).
- ³I. Benjamin, Annu. Rev. Phys. Chem. **66**, 165 (2015).
- ⁴G. Gonella, E. H. Backus, Y. Nagata, D. J. Bonthuis, P. Loche, A. Schlaich, R. R. Netz, A. Kühnle, I. T. McCrum, M. T. Koper *et al.*, Nat. Rev. Chem. 5, 466 (2021).
 ⁵M. F. Ruiz-Lopez, J. S. Francisco, M. T. Martins-Costa, and J. M. Anglada, Nat. Rev. Chem. 4, 459 (2020).
- ⁶M. T. Martins-Costa and M. F. Ruiz-López, J. Phys. Chem. B 117, 12469 (2013).
- ⁷K. Piradashvili, E. M. Alexandrino, F. R. Wurm, and K. Landfester, Chem. Rev. 116, 2141 (2016).
- ⁸S. Hosseinpour, S. J. Roeters, M. Bonn, W. Peukert, S. Woutersen, and T. Weidner, Chem. Rev. **120**, 3420 (2020).
- ⁹A. Zgorski, R. W. Pastor, and E. Lyman, J. Chem. Theory Comput. 15, 6471 (2019).
- ¹⁰C. V. Sternling and L. E. Scriven, AIChE J. 5, 514 (1959).
- ¹¹ M. J. Boussinesq, Ann. Chim. Phys **29**, 349 (1913).

- ¹²L. E. Scriven, Chem. Eng. Sci. **12**, 98 (1960).
- ¹³ B. Scheid, J. Delacotte, B. Dollet, E. Rio, F. Restagno, E. A. van Nierop, I. Cantat, D. Langevin, and H. A. Stone, Europhys. Lett. **90**, 24002 (2010).
- ¹⁴H. A. Stone and L. G. Leal, J. Fluid Mech. **220**, 161 (1990).
- ¹⁵G. J. Elfring, L. G. Leal, and T. M. Squires, J. Fluid Mech. **792**, 712 (2016).
- ¹⁶J. C. Earnshaw, Nature **292**, 138 (1981).
- ¹⁷ J. C. Earnshaw and C. J. Hughes, Langmuir 7, 2419 (1991).
- ¹⁸B. Fábián, M. Sega, G. Horvai, and P. Jedlovszky, J. Phys. Chem. B **121**, 5582 (2017).
- ¹⁹P. Malgaretti, U. Bafile, R. Vallauri, P. Jedlovszky, and M. Sega, J. Chem. Phys. 158, 114705 (2023).
- ²⁰S. Narayan, J. Muldoon, M. G. Finn, V. V. Fokin, H. C. Kolb, and K. B. Sharpless, Angew. Chem., Int. Ed. 44, 3275 (2005).
- ²¹ Y. Jung and R. A. Marcus, J. Am. Chem. Soc. **129**, 5492 (2007).
- ²²R. Kubo, J. Phys. Soc. Jpn. **12**, 570 (1957).
- ²³B. Hess, J. Chem. Phys. **116**, 209 (2002).
- $^{\mathbf{24}}$ D. Duque-Zumajo, J. De La Torre, and P. Español, J. Chem. Phys. **152**, 174108 (2020).
- ²⁵ M. Sega, B. Fábián, and P. Jedlovszky, J. Chem. Phys. **143**, 114709 (2015).
- ²⁶J. E. Fitzgerald, R. M. Venable, R. W. Pastor, and E. R. Lyman, Biophys. J. **122**, 1094 (2023).
- ²⁷ M. J. Abraham, T. Murtola, R. Schulz, S. Páll, J. C. Smith, B. Hess, and E. Lindahl, SoftwareX 1–2, 19 (2015).
- ²⁸S. Nosé, Mol. Phys. **52**, 255 (1984).
- ²⁹W. G. Hoover, Phys. Rev. A 31, 1695 (1985).
- ³⁰P. J. in 't Veld, A. E. Ismail, and G. S. Grest, J. Chem. Phys. **127**, 144711 (2007).
- ³¹C. L. Wennberg, T. Murtola, S. Páll, M. J. Abraham, B. Hess, and E. Lindahl, J. Chem. Theory Comput. 11, 5737 (2015).
- ³²U. Essmann, L. Perera, M. L. Berkowitz, T. Darden, H. Lee, and L. G. Pedersen, J. Chem. Phys. **103**, 8577 (1995).
- ³³ M. Sega, S. S. Kantorovich, P. Jedlovszky, and M. Jorge, J. Chem. Phys. **138**, 044110 (2013).
- ³⁴ M. Sega, G. Hantal, B. Fábián, and P. Jedlovszky, J. Comput. Chem. 39, 2118 (2018).
- 35 G. Hantal, P. Jedlovszky, and M. Sega, Soft Matter 19, 3773 (2023).
- ³⁶E. W. Lemmon and R. T. Jacobsen, Int. J. Thermophys. 25, 21 (2004).